Supporting Information

Folded-Twisted Mechanisms Control Dynamic Redox Properties, Photophysics and Electron Transfer of Antha nthrene-Quinodimethanes

Abel Cárdenas Valdivia,[‡a] Frédéric Lirette,[‡b] José Marín-Beloqui,[*a] Abel Carreras,[*c] David Casanova,[de] Joël Boismenu-Lavoie,[b] Jean-François Morin,[b,*] Juan Casado,[*a]

[a]Department of Physical Chemistry, University of Málaga, Andalucia-Tech, Campus de Teatinos s/n, 29071 Málaga, Spain. E-mail: casado@uma.es

[b]Département de Chimie, Université Laval, 1045 Ave de la Médecine, Québec, Canada G1V 0A6

[c]Multiverse Computing, 20014 Donostia, Euskadi, Spain

[d]Donostia International Physics Center (DIPC), 20018 Donostia, Euskadi, Spain

[e]IKERBASQUE - Basque Foundation for Science, 48009 Bilbao, Euskadi, Spain

‡ These authors contribute equally to the article

Synthesis

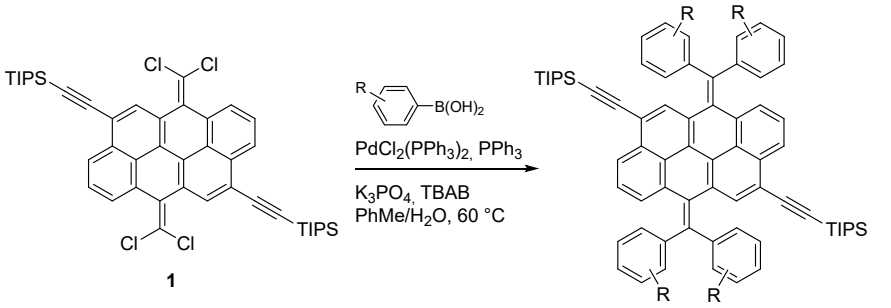

Scheme S1. Cyclic voltammograms cycles of A(*m*-OMe, blue line) at 298 K at a scan rate of 100 mV/s in 0.1 M TBAPF in CH_2Cl_2. Potentials have been corrected using ferrocene as reference.

Compound A(*m*-OMe)

A screw-capped pressure vessel under nitrogen was charged with compound **1** (300 mg, 0.38 mmol), 3-methoxyphenylboronic acid (456 mg, 3.0 mmol), tripotassium phosphate (1.27 g, 6.00 mmol), tetrabutylammonium bromide (60 mg, 0.19 mmol), bis(triphenylphosphine)palladium(II) chloride (53 mg, 0.08 mmol) and triphenylphosphine (25 mg, 0.09 mmol). The mixture was purged and degassed with a flow of nitrogen for 30 min. Degassed toluene (36 mL) and degassed water (3 mL) were added. The mixture was heated at 60 °C for 16h, protected from light then diluted in dichloromethane and washed three times with water. The organic layer was dried over $MgSO_4$ and the solvent was removed under reduced pressure. The crude product was purified by silica gel column chromatography (DCM/hexanes 1:1 v/v) to afford the desired compound as orange flakes (332 mg, 81%).

^{1}H NMR (400 MHz, $CDCl_3$, 55 °C) δ 8.02 (dd, J = 8.1, 1.1 Hz, 2H), 7.57 (s, 2H), 7.41 (dd, J = 7.5, 1.1 Hz, 2H), 7.18-7.26 (m, 4H), 7.12 (t, J = 7.8 Hz, 2H), 7.06 (d, J = 7.7 Hz, 2H), 7.02 – 6.84 (m, 6H), 6.76 (t, J = 7.4 Hz, 4H), 3.76 (s, 2H), 3.74 (s, 2H) 1.14 (s, 42H).

^{13}C NMR (101 MHz, $CDCl_3$) δ 159.97, 159.71, 144.78, 144.59, 143.25, 133.37, 132.79, 132.25, 131.23, 130.86, 129.91, 129.68, 128.68, 127.57, 127.12, 125.65, 125.14, 122.28, 121.96, 119.33, 115.62, 115.39, 112.08, 111.92, 105.33, 95.46, 77.32, 77.00, 76.68, 55.19, 18.77, 11.36.

HRMS (APPI+) : $C_{74}H_{79}O_4Si_2$ $[M+H]^+$ 1087.5517; found, 1087.5511

Compound A(*p*-F)

A screw-capped pressure vessel under nitrogen was charged with compound **1** (100 mg, 0.12 mmol), 4-fluorophenylboronic acid (224 mg, 1.01 mmol), tripotassium phosphate (424 mg, 2.00 mmol), tetrabutylammonium bromide (20 mg, 0.06 mmol), bis(triphenylphosphine)palladium(II) chloride (18 mg, 0.025 mmol) and triphenylphosphine (7 mg, 0.03 mmol). The mixture was purged and degassed with a flow of nitrogen for 30 min. Degassed toluene (12 mL) and degassed water (1 mL) were added. The mixture was heated at 60 °C for 16h, protected from light then diluted in dichloromethane and washed three times with water. The organic layer was dried over $MgSO_4$ and the solvent was removed under reduced pressure. The crude product was purified by silica gel column chromatography (DCM/ hexanes 4:1 v/v) to afford the desired compound as a yellow powder (111 mg, 85%).

^{1}H NMR (500 MHz, $CDCl_3$) δ 8.06 (dd, *J* = 8.2, 1.1 Hz, 2H), 7.48 (s, 2H), 7.41 – 7.23 (m, 10H), 7.15 (s, 2H), 7.02 (t, *J* = 8.5 Hz, 8H), 1.16 (d, *J* = 1.5 Hz, 42H).

^{13}C NMR (126 MHz, $CDCl_3$, 50 °C) δ 163.11, 161.14, 141.86, 139.52, 133.59, 133.52, 132.96, 131.61, 131.59, 131.55, 131.03, 129.09, 127.85, 127.42, 125.99, 125.72, 120.01, 116.17, 116.01, 105.23, 96.64, 18.89, 11.63.

HRMS (APPI+) : C70H66Si2F4 $[M^*]^+$ 1038.4639; found, 1038.4655

Experimental Details

Chemicals and reagents were purchased from commercial suppliers and used as received.

Cyclic voltammetry (CV) measurements were performed in dry DCM on a commercial instrument with a three-electrode cell, using 0.1 M Bu_4NPF_6 as supporting electrolyte, AgCl/Ag as reference electrode, gold disk as working electrode, Pt wire as counter electrode, and scan rate at 50 mV/s. The potential was externally calibrated against the ferrocene/ferrocenium couple

Spectroelectrochemistry has been conducted on the Varian Cary 5000 UV-Vis-NIR spectrophotometer while the voltage was applied by a C3 epsilon potentiostat from BASi using a thin layer cell from a demountable omni cell from Specac. In this cell a three electrodes system was coupled to conduct in situ spectroelectrochemistry. A Pt gauze was used as the working electrode, a Pt wire was used as the counter electrode, and an Ag wire was used as the pseudo-reference electrode. The spectra were collected a constant potential electrolysis and the potentials were changed in interval of 10 mV. The electrochemical medium used was 0.1 M tetrabutyl ammonium hexafluorophosphate, Bu_4NPF_6, in fresh distilled dichloromethane, at room temperature with sample concentrations of 10^{-3} M.

The temperature-dependent variation in the absorption spectrum of the dications was measured by following the next procedure. First, the compounds were chemically oxidised using $FeCl_3$.Then, the solution was transferred to a cryostat OPTISTAT from Oxford instruments to perform the characterisation with the Varian Cary 5000 UV-Vis-NIR spectrophotometer.

Emission was measured using a spectrofluorometer from Edinburgh Analytical Instrument (FLS920P) equipped with a pulsed xenon flash-lamp, Xe900, of 400 mW.

Picosecond transient absorption spectra were obtained using a Helios system from Ultrafast Systems. This setup includes an amplified femtosecond Spectra-Physics Solstice-100F laser, featuring a 128 fs pulse width and a 1 kHz repetition rate, coupled with a Spectra-Physics TOPAS Prime F optical parametric amplifier, covering a range of 195-22000 nm.

Microsecond transient absorption spectroscopy was measured in fresh degassed *ca.* 10^{-3} M solutions at room temperature by means of a laser flash photolysis system from Luzchem with a pulsed Nd:YAG laser, using 532 nm excitation wavelength. Probe light was provided by a Lo255 Oriel xenon lamp. The apparatus is completed with a 77200 Oriel monochromator, an Oriel photomultiplier (PMT) system and a TDS-640A Tektronix oscilloscope. The energy single pulses were of *ca.* 15 mJ.

Variable temperature experiments where temperature was decreased to 80 were done using 2-methyl-tetrahydrofuran (2-Me-THF, Sigma-Aldrich/Merck, Anhydrous, ≥99%) ca. 10^{-5} M solutions.

Computational details

Molecular geometries were optimized with the density functional theory (DFT) in conjunction with the CAM-B3LYP exchange-correlation functional [Chem. Phys. Lett., 2004, 393, 51-57] and the 6-31G(d,p) basis set. Low-lying states were obtained using (linear response) time-dependent DFT (TDDFT) within the Tamm–Dancoff approximation (TDA) [Chem. Phys. Lett. 1999, 314, 291-299] and the same functional and basis set. Absorption spectra were simulated by convolution of Gaussian functions added at each computed vertical excitation with a half-with at half maximum (HWHM) of 0.1 eV. Spin-orbit couplings (SOCs) where obtained at the same level of theory considering and by means of the one-electron part of the Breit-Pauli Hamiltonian.

All electronic structure calculations were performed with the Q-Chem package [J. Chem. Phys. 2021, 155, 084801].

Table S1. Highest occupied molecular orbital (HOMO) and Lowest unoccupied molecular orbital (LUMO) energies (in eV) computed for the folded and twisted forms of **A(*m*-OMe)** and **A(*p*-F)**.

	A(*p*-F)		A(*m*-OMe)	
	Folded	**Twisted**	**Folded**	**Twisted**
LUMO	-2.434	-2.635	-2.352	-2.632
HOMO	-5.068	-4.580	-5.053	-4.573

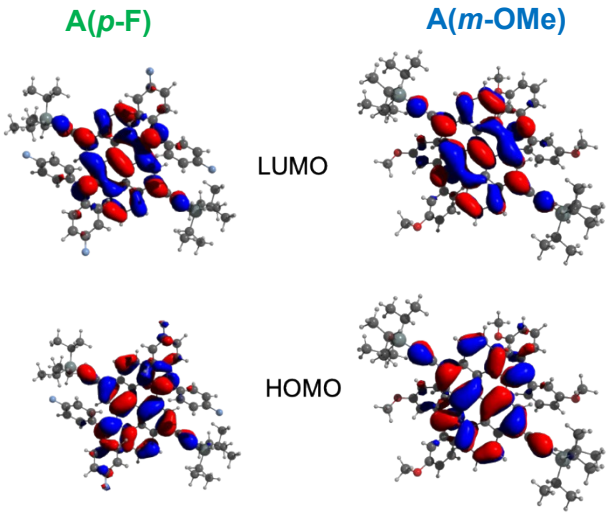

Figure S1. HOMO and LUMO of **A(*m*-OMe)** and **A(*p*-F)** molecules in the folded forms.

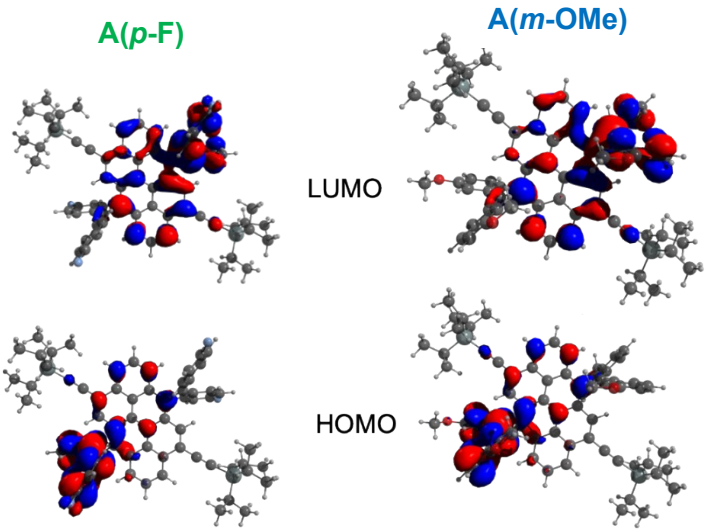

Figure S2. HOMO and LUMO of **A(*m*-OMe)** and **A(*p*-F)** molecules in the twisted open-shell forms.

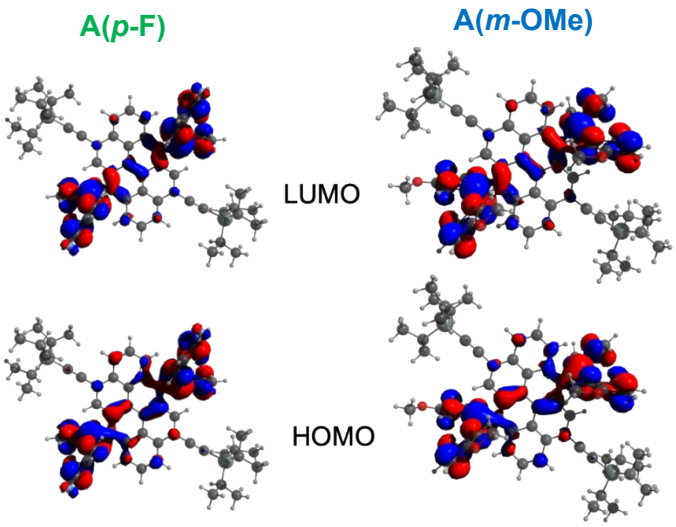

Figure S3. HOMO and LUMO of **A(*m*-OMe)** and **A(*p*-F)** molecules in the twisted closed-shell forms.

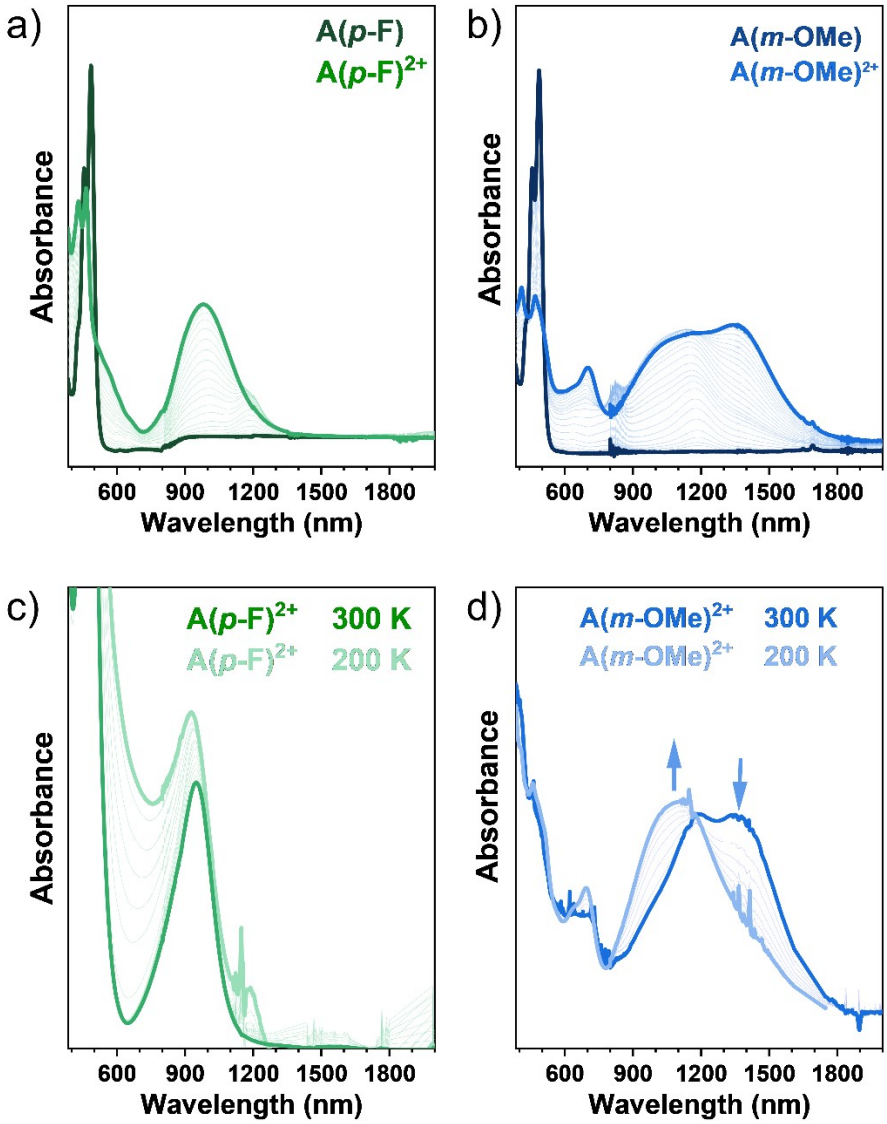

Figure S4. Spectroelectroabsorption spectra of **a) A(*m*-OMe)** and **b) A(*p*-F)** in 0.1 M $TBAPF_6$ in CH_2Cl_2 at room temperature. Temperature evolution of **c) A(*m*-OMe)** and **d) A(*p*-F)** dications from 300 to 200K.

In the oxidation process of **A(*p*-F)** at low oxidation potentials, the formation of a band at 1200 nm is seen in Figure S2a which quickly disappears after increasing oxidation. The appearance of this band can result from the radical cation formed by a disproportion reaction at low potentials where the concentration of neutral species in the Nernst layer is still significant.

$$\mathbf{A(\mathit{p}\text{-F})} + \mathbf{A(\mathit{p}\text{-F})^{+2}} \rightarrow 2\ \mathbf{A(\mathit{p}\text{-F})}\ \mathbf{A(\mathit{p}\text{-F})^{+\bullet}}$$

When the potential is increased the direct massive formation of the dication minimizes the disproportion reaction effect.

A similar disproportion reaction also takes place for the initial oxidation at low potentials of **A(*m*-OMe)** at which a starting rise of the 1200 nm band occurs (radical cation) followed by the overhelming appearance of the 1350 nm band of the dication.

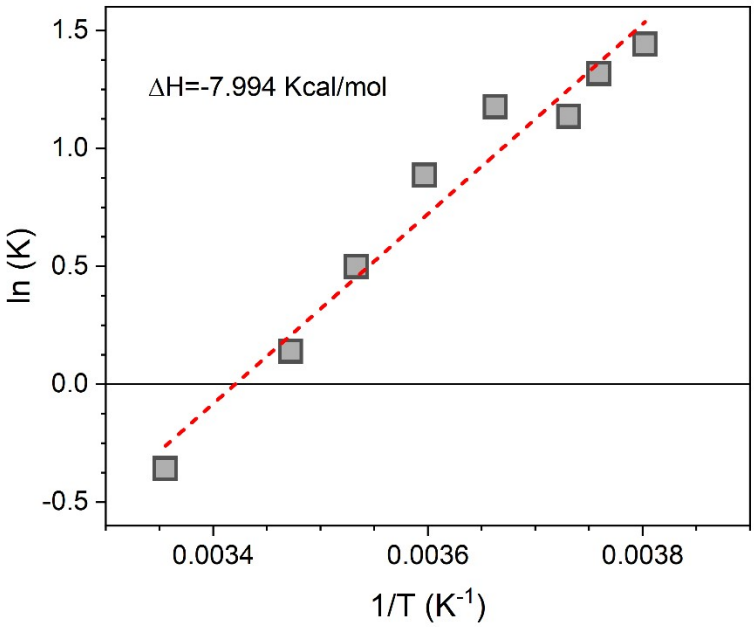

Figure S5. Van´t Hoff plot for the equilibrium between folded and twisted **A(*m*-OMe)$^{2+}$** conformers by using the absorbance at variable temperature of the dicationic species.

The van´t Hoff equation relates the changes in the equilibrium constant with the changes in temperature. For a small variation of temperature, to maintain the standard entropy variation constant this equation is:

$$ln(K_{eq}) = \frac{\Delta H^{\circ}}{R}\left(\frac{1}{T}\right)$$

where K_{eq}, ΔH^{o}, R and T are the equilibrium constant, the standard enthalpy variation, the ideal gas constant and the temperature, respectively.

To construct the van´t Hoff plot, we calculate the K_{eq} for each temperature in our system. To calculate it, we fit the absorbance spectra at each temperature to the equilibrium of two gaussian, where the area under each gaussian corresponds to the concentration of each reactant according to the Lambert-Beer law. For the equilibrium transformation from the twisted conformation (with a band centred at 1365 nm) to the folded conformation (with a band seen at 1110 nm), as shown the Figure 2a, we integrate the gaussian fittings of these two bands, considering the folded conformer as the product of the equilibrium.

Then, we fit the van´t Hoff plot to a line where the slope is related with the standard enthalpy variation, which we estimated as -7.994 Kcal/mol.

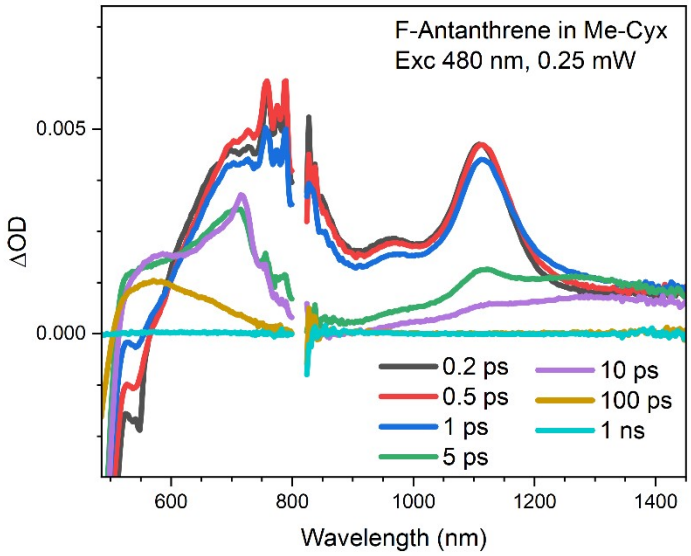

Figure S6. Femtosecond transient absorption measurements of pristine **A(*p*-F)** in methylcyclohexane after pumping at 480 nm. Excitation densities were maintained at 0.25 mW.

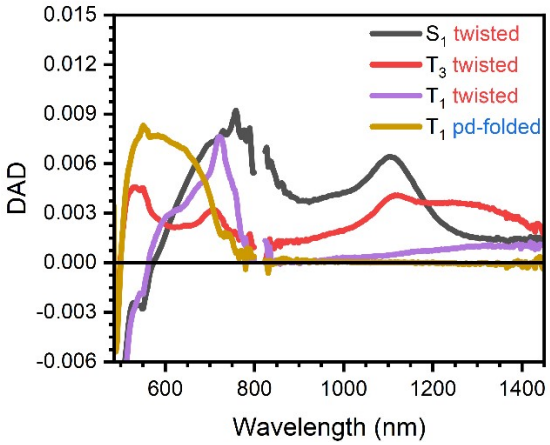

Figure S7. Decay associated spectra of the different species obtained by the global analysis performed on the ps-TAS results of **A(*m*-OMe)** in methycyclohexane.

Table S2. Singlet-triplet energy differences (in eV) and SOC constants (SOCCs in cm-1) between S_1 and T_n states at the S_1 optimized geometry (twisted conformation) of **A(m-OMe)** computed at the CAM-B3LYP/6-31G(d,p) level.

T_n state	$E(S_1)$-$E(T_n)$	SOCC
T_1	1.46	0.03
T_2	0.43	2.15
T_3	0.02	0.70
T_4	-0.49	0.15
T_5	-0.64	0.18
T_6	-0.75	0.24
T_7	-0.85	0.70

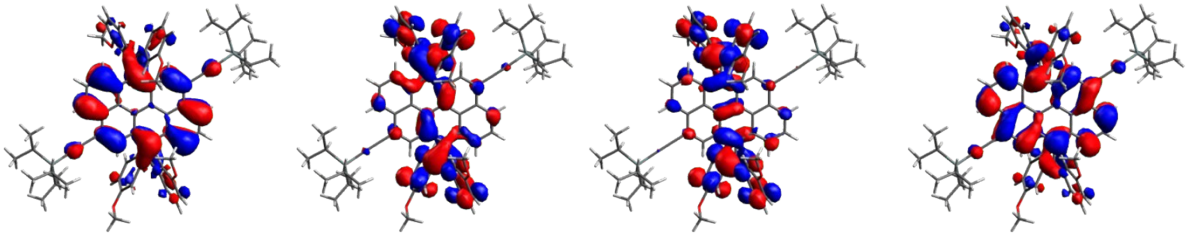

Figure S8. Frontier molecular orbitals describing the electronic structure of singlet and triplet states (S_1 and T_3) potentially involved in the ISC of **A(m-OMe)** at the S_1 optimized geometry (twisted conformation). Both states are mainly obtained as HOMO-1 → LUMO and HOMO → LUMO+1 transitions.

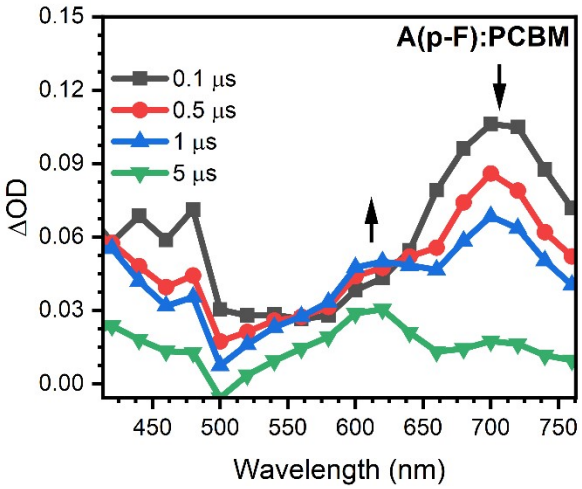

Figure S9. TA spectra of a **A(*p*-F)** solution obtained at 0.1 (black squares), 0.5 (red circles), 1 (blue triangles) and 5 μs (green inverted triangles) upon 532 nm laser excitation.

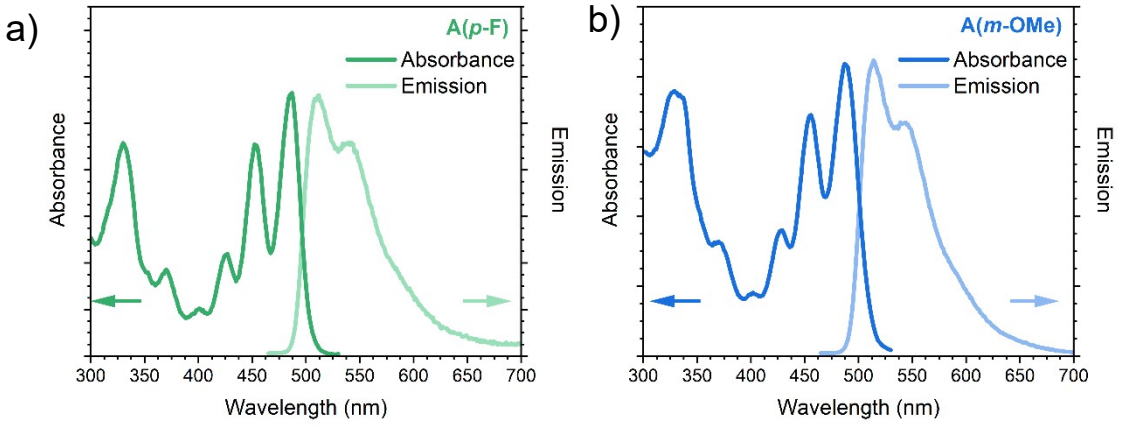

Figure S10. Normalized ground state absorbance (darker lines) and steady-state emission (lighter lines) spectra for **a) A(*p*-F)** and **b) A(*m*-OMe)** 2-MeTHF solution at 80 K.

NMR spectra

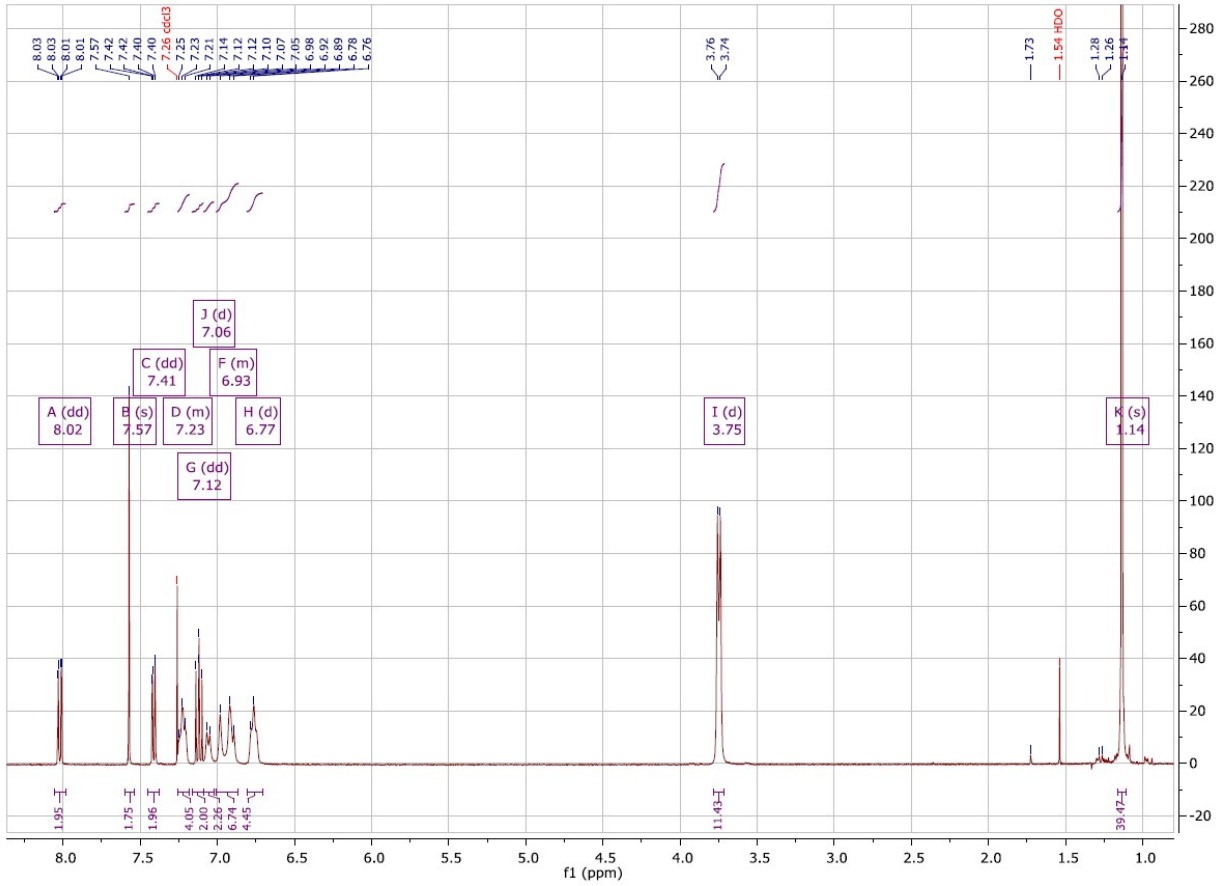

Figure S11. ^{1}H NMR (400 MHz) of compound **A(*m*-Ome)** in $CDCl_3$ at 55 °C.

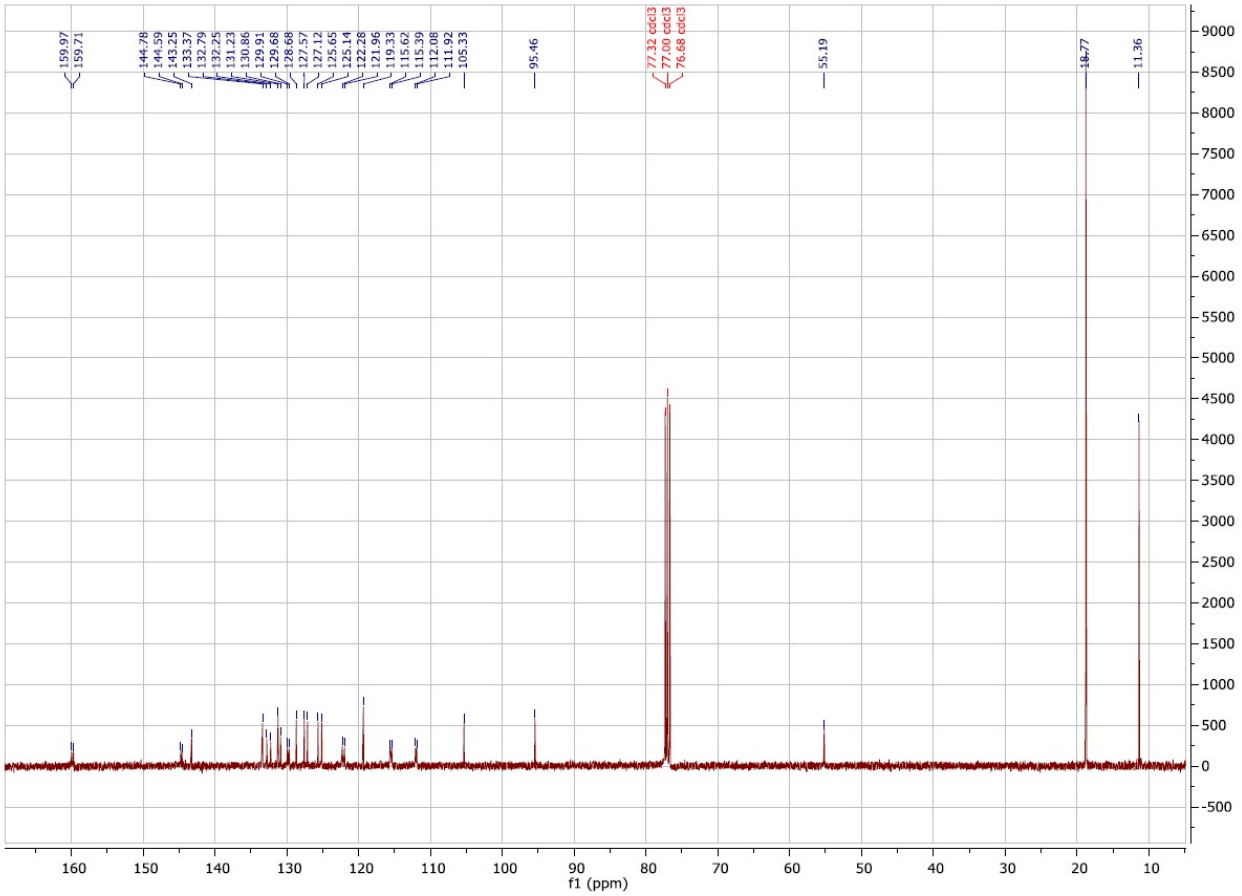

Figure S12. ^{13}C NMR (101 MHz) of compound **A(*m*-Ome)** in $CDCl_3$ at 55 °C.

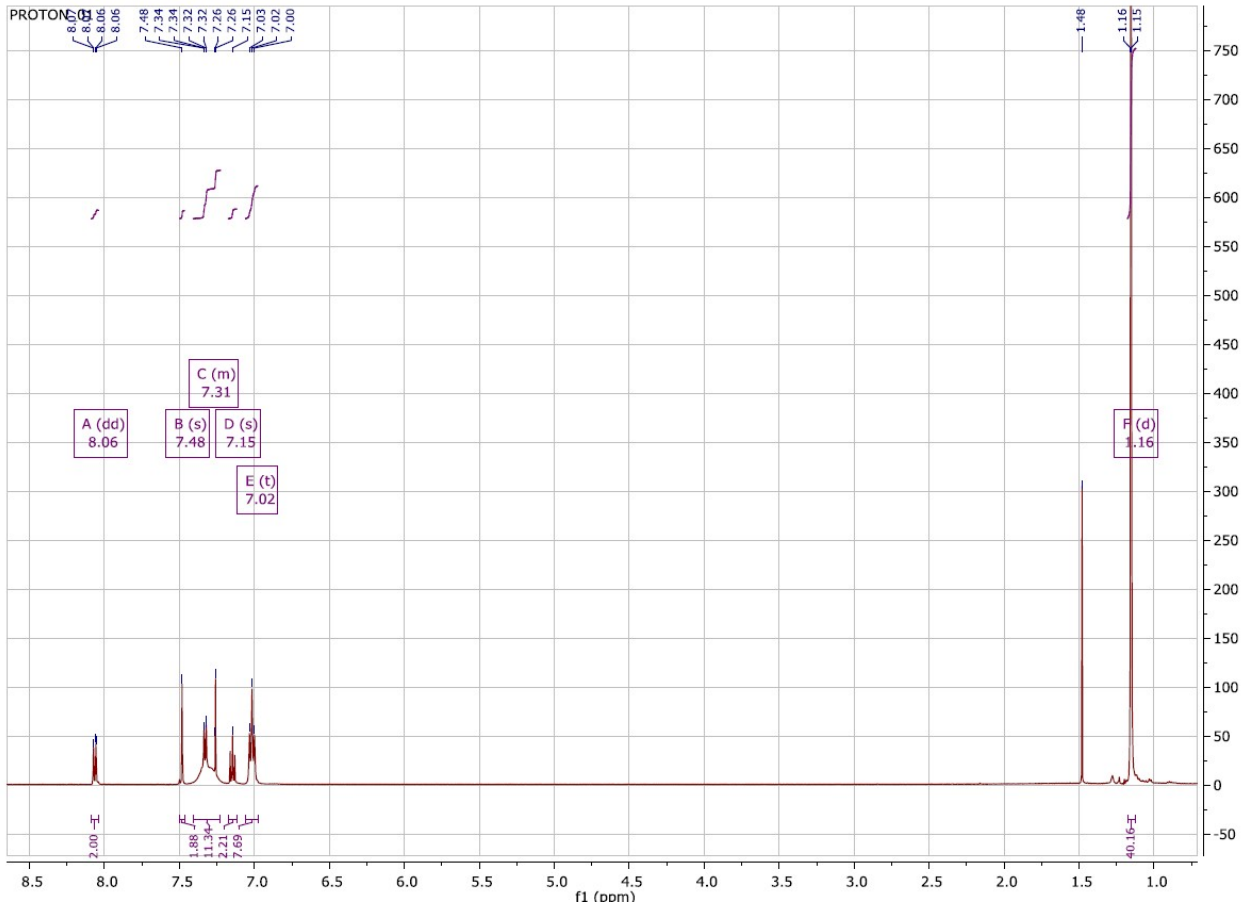

Figure S13: ^{1}H NMR (400 MHz) of compound **A(*p*-F)** in $CDCl_3$ at 25 °C.

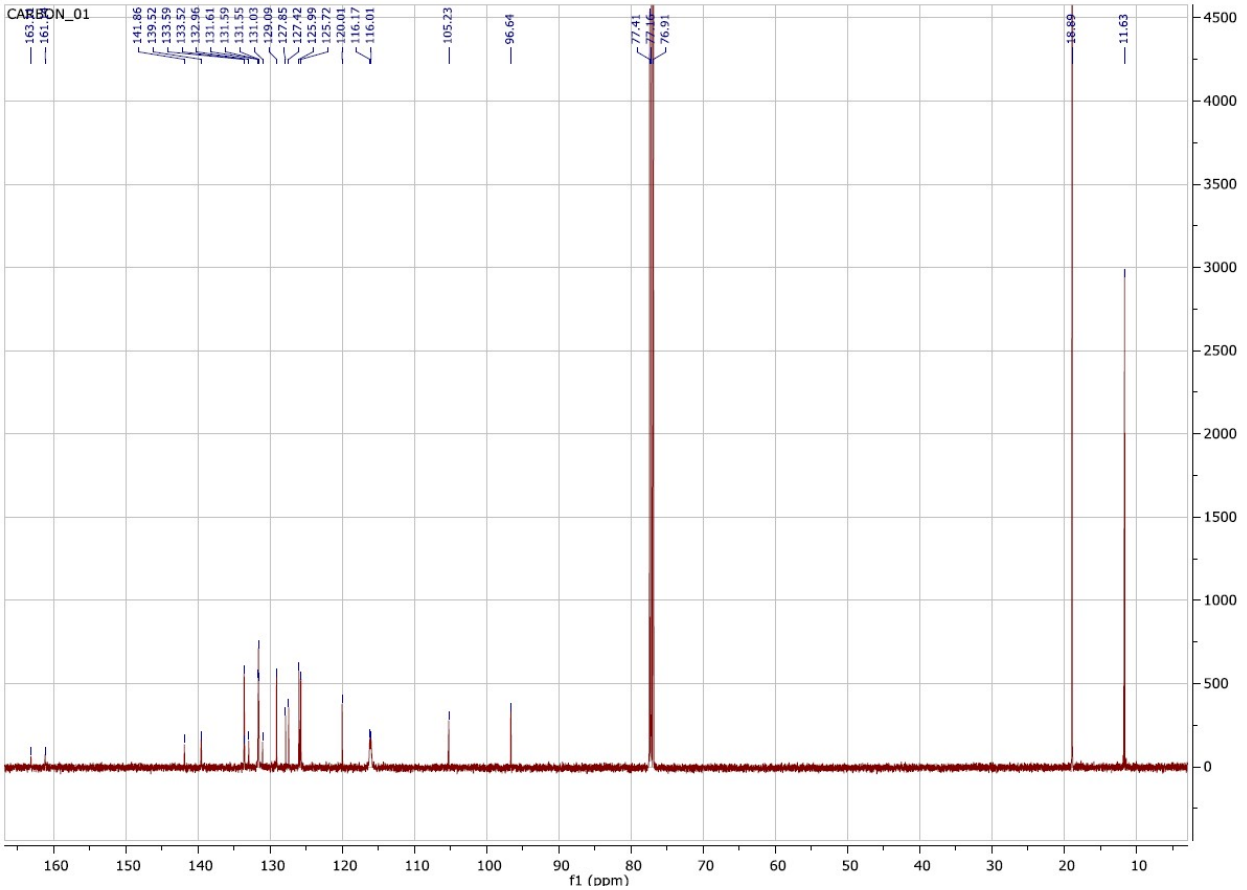

Figure S14. ^{13}C NMR (101 MHz) of compound **A(*p*-F)** in $CDCl_3$ at 25 °C.